

## Dynamic mechanical analysis of the multiple glass transitions of plasticized wheat gluten biopolymer

Antoine Duval,<sup>1,2,3,4</sup> Sonia Molina-Boisseau,<sup>1,2</sup> Christine Chirat,<sup>3,4</sup> Marie-Hélène Morel<sup>5</sup>

<sup>1</sup>CERMAV, Univ. Grenoble Alpes, Grenoble F-38000, France

<sup>2</sup>CERMAV, CNRS, Grenoble F-38000, France

<sup>3</sup>Univ. Grenoble Alpes, LGP2, Grenoble F-38000, France

<sup>4</sup>CNRS, LGP2, Grenoble F-38000, France

<sup>5</sup>UMR IATE, UM2-CIRAD-INRA-SupAgro, 2 Pl Pierre Viala, Montpellier 34070, France

Correspondence to: S. Molina-Boisseau (E-mail: sonia.boisseau@cermav.cnrs.fr)

**ABSTRACT:** Glass transition of thermo-molded biomaterials made from wheat gluten and its main protein classes is studied by dynamic mechanical analysis (DMA). The materials are plasticized with variable contents of glycerol (30–40 wt %) and water (0–20 wt %). For all materials, three successive relaxation phases are systematically detected. Their positions shift to lower temperature as the plasticizer content of materials increases. Composition in gluten, glycerol and water of each relaxation phase is estimated using the Couchman-Karas model. Irrespective of the plasticizer content or composition, the relaxation phases shows rather constant plasticizer volume fractions. The low-, middle-, and high relaxation phases include respectively around 30, 60 and 80 vol % of gluten protein. These relaxations are assigned to the segmental motion of the surface amino-acid side groups, to the collective motion of packed gluten proteins, and to the gain in protein conformational mobility as a 2D network of interacting plasticizer molecules forms. © 2015 Wiley Periodicals, Inc. *J. Appl. Polym. Sci.* **2016**, *133*, 43254.

**KEYWORDS:** biopolymers and renewable polymers glass transition; plasticizer; proteins

Received 15 June 2015; accepted 23 November 2015

DOI: 10.1002/app.43254

### INTRODUCTION

The use of polymers from renewable resources is often presented as a way to decrease the consumption of ordinary petroleum-based, non-biodegradable plastics, and to reduce the environmental footprint of manufactured products. Different types of biopolymers can be extracted from a wide variety of agricultural, forestry or marine products.<sup>1,2</sup> Plant proteins, such as wheat gluten (WG), soy protein isolate or zein, constitute a class of interest for material applications, because they are available in large amount, as by-products of wheat, soy and corn refining industries respectively, and still don't have many industrial applications.<sup>3</sup> These protein sources can be processed into materials, and several recent reviews summarize their main properties.<sup>3–5</sup> WG is, together with soy protein isolate, the one that has retained the most attention, and constitutes the purpose of this study.

Like most biopolymers, proteins bear high amount of pendant hydrogen donor or acceptor groups, such as hydroxyls, amino or carboxyl groups, which allow the formation of inter- and intramolecular hydrogen bonds. The latter contributes to their

folding stability whereas the complementary hydrogen-bonding groups on biopolymer surfaces promote self-assembly and confer additional rigidity. WG includes two main protein classes, gliadin and glutenin, which share similar amino-acid composition but differ in molecular size.<sup>6</sup> Gliadins, which typically account for 40 to 50 wt % of gluten, consist of a blend of monomeric polypeptides, whose molar masses range from 30,000 to 80,000 g mol<sup>-1</sup>.<sup>7,8</sup> Glutenins result from the concatenation of several polypeptides (i.e. subunits), through inter-chain disulfide bonds. Glutenin size distribution is quite large, from 100 000 to several millions g mol<sup>-1</sup>.<sup>8–10</sup> Despite their very large difference in molecular size, the glass transition temperature of dry gliadin and glutenin estimated from DSC analysis were reported to fall within the same range from 138 to 145°C<sup>11,12</sup> or 162 to 173°C.<sup>13</sup>

Processing proteins above their glass transition temperature is impossible because irreversible degradation of amino-acid side chain sharply rises above 200°C. To overcome this limitation, plasticizers are used. The purpose is to reduce the polymer–

Additional Supporting Information may be found in the online version of this article.

© 2015 Wiley Periodicals, Inc.

polymer inter-chain interactions, by replacing them by polymer-plasticizer interactions. This results in enhanced chain mobility, and lower  $T_g$ .<sup>14,15</sup> Plasticizers strongly impact the physical properties of the polymers around the ambient temperature: the rigidity and the mechanical strength are reduced, whereas the ductility is enhanced.<sup>16–19</sup> Water sensitivity and gas permeability are also affected.<sup>18–20</sup>

The plasticizer performance depends on a right balance between its capability to reduce the  $T_g$  of the polymer phase while being chemically compatible with it. Chemical compatibility with polymer chains prevents for phase segregation and guarantees plasticizer long term action. Many parameters can influence it, such as the chemical composition and structure of the plasticizer, its molar mass, or its polarity.<sup>14,15</sup> As for most biopolymers, the plasticization of WG can be achieved by using molecules able to form hydrogen bonds.<sup>21</sup> Polyols are routinely used (glycerol,<sup>21,22</sup> sorbitol,<sup>22</sup> 1,4-butanediol,<sup>21</sup> ethylene or propylene glycol and their oligomers, di- and triethanolamine<sup>23</sup>...), but some studies also investigated the effectiveness of e.g., lactic acid,<sup>21</sup> fatty acids or amide compounds.<sup>24</sup>

Because of its high content in hydrophilic groups, WG is efficiently plasticized by water and very sensitive to moisture changes. The water retention capacity of WG materials is further enhanced in the presence of hydrophilic plasticizers.<sup>19</sup> When stored in moist environments, glycerol-plasticized WG materials are in fact ternary blends of glycerol, gluten and water. To understand the plasticization of WG by glycerol, it is thus necessary to study the co-influence of both water and glycerol.

Two main approaches can be used to measure the glass transition of polymeric materials. Differential scanning calorimetry (DSC) gives the true glass transition temperature  $T_g$ , identifiable as a change in the slope of the heat capacity vs. temperature. Dynamic mechanical analysis (DMA) gives on the other hand a dynamic transition temperature, based on the evolution of the complex modulus with the temperature, rigorously denominated as  $T_\alpha$ . However, the  $T_\alpha$  can also be considered to represent the glass transition, and it is quite common in the literature to discuss glass transition data based on DMA experiments.

For miscible binary mixtures of polymer and plasticizer, the  $T_g$  of the blend varies with the plasticizer content in a monotonic manner, predictable through established models. Hence, the Couchman-Karasz (C-K) model allows the prediction of the glass transition temperature of blends of known composition, from the specific  $T_g$  and changes in heat capacity ( $\Delta C_p$ ) of the components.<sup>25</sup> The model still applies for ternary mixtures involving two different plasticizers.<sup>26,27</sup> C-K equation is well adapted to predict variation of the  $T_g$  of biomaterials including hygroscopic plasticizers like polyols. It is traditionally admitted that multiple glass transitions refer to the separated phases coexisting in non-miscible polymer and plasticizer blends. However, multiple glass transition would also reflect distinct local environments of more or less mobile (i.e., plasticized) molecular clusters, either rich or poor in one of the system components.

Thermal processing of WG into materials induces drastic changes in the proteins organization: glutenin polymers are

highly sensitive to thermal denaturation above 60°C which leads to their assembly into disulfide bonded aggregates. Gliadins, lacking free thiol groups, are less prone to aggregation through thiol/disulfide exchanges.<sup>28–30</sup> However, during thermal treatment gliadin interact with glutenin, and both gluten protein classes become strongly insolubilized by thermal treatment.<sup>31,32</sup> How the plasticizer content impacts gluten protein crosslinking remained poorly documented, but it is admitted that glycerol content around 30 wt % allows the production of materials showing good mechanical strength at room temperature.

In this study, we prepared materials based on WG and its different protein classes, using various amounts of glycerol as plasticizer. Storage of the films at different relative humidities (RH) resulted in different effective water contents, and the thermal relaxation of the materials was evaluated using DMA. The aim is to evaluate the co-influence of glycerol and water on the complex shape of the  $\tan \delta$  curves measured by DMA, and to give new insights on the dynamical heterogeneities of gluten-biomaterials plasticized by a blend of hydrophilic plasticizers.

## EXPERIMENTAL

### Materials

WG was supplied by Tereos Syral (Marckolsheim, France). Its moisture content, measured after 24 h drying at 105°C, was 12.4 wt %. Glycerol (reagent grade, >99.0%) was purchased from Sigma-Aldrich and used as received.

### Fractionation of Wheat Gluten

The fractionation of WG into gliadin- and glutenin-rich fractions has been conducted according to Chen *et al.*<sup>33</sup> Briefly, 36 g pre-dried WG was suspended overnight in 180 mL ethanol solution (70 vol %) at room temperature. The soluble and insoluble fractions were separated by centrifugation. The insoluble fraction was re-suspended in fresh ethanol solution and treated as before. The soluble fractions from both extractions were combined, evaporated to dryness in a rotary evaporator, washed with water and freeze-dried to yield the gliadin-rich fraction. The insoluble fraction was washed with water and freeze-dried to yield the glutenin-rich fraction.

### Characterization of Protein Fractions

The nitrogen content was obtained by elementary analysis, performed at Service Central d'Analyse (CNRS, Villeurbanne, France). The protein content was then obtained as  $N$  (wt %)  $\times$  5.7.

The starch content was measured by spectrophotometric titration using  $I_2$  as complexing agent, as described by Jarvis and Walker.<sup>34</sup>

The gliadin and glutenin content of the samples were determined by size exclusion high performance liquid chromatography (SE-HPLC). The samples were prepared as described by Domenek *et al.*<sup>35</sup> Briefly, the samples were first extracted in the presence of a surfactant, sodium dodecyl sulfate (SDS), resulting in the solubilization of monomeric gliadins and part of the polymeric glutenins. Then, a second extraction is performed by adding dithioerythriol (DTE), a reducing agent able to disrupt the disulfide bonds and to solubilize the resulting glutenin subunits.

**Table I.** Composition of the Protein Samples (Dry Basis)

	On total weight				On protein weight	
	Yield (%)	N (%)	Protein (%)	Starch (%)	Gliadin (%)	Glutenin (%)
Gluten	–	13.4	76.4	19.4 ± 0.4	56.0	44.1
Gliadin-rich	23.7 ± 3.6	14.5	82.7	1.6 ± 0.2	85.2	14.8
Glutenin-rich	56.3 ± 2.0	13.6	77.5	7.5 ± 0.2	36.7	63.1

The extracts were further injected on a SE-HPLC system equipped with an analytical column TSK-G 4000-SWXL (7.8 × 300 mm, Tosoh Biosep), coupled to a guard column TSK SWXL (6 × 40 mm, Tosoh Biosep). They were eluted at room temperature by pH 6.9 phosphate buffer containing 0.1 wt % SDS, at 0.7 mL min<sup>-1</sup>. The proteins were detected by UV absorbance at 214 nm.

The chromatogram of the first extract is divided into five fractions, according to Morel *et al.*,<sup>29</sup> and the areas are quantified. The gliadin content can be obtained as the area of the fractions F3 to F5, whereas the glutenin content is obtained by adding the area of fractions F1 and F2 to the total area of the chromatogram of the second extract.

#### Elaboration of Materials

The protein powder (gluten, gliadin- or glutenin-rich fraction) was first mixed with glycerol (30, 35 or 40 wt % based on total dry weight) in a two-blade counter-rotating batch mixer, turning at 3:2 differential speed (Brabender, Duisburg, Germany). Mixing was performed for 15 min, at a mixing speed of 100 rpm and a regulation temperature set at 70°C. The use of a 70–80°C regulation temperature range was found to limit the induction period needed to develop a cohesive WG-glycerol material in 3:2 batch mixer.<sup>36</sup> Glycerol was first introduced into the chamber, as it provides more homogeneous blends.

The blends were then thermo-molded in a heated press (Carver laboratory press, Carver Inc, Menomonee Falls, WI) at 120°C. Approximately 4 g of polymer blends were placed between two aluminum sheets in a rectangular mold (8 × 4 cm<sup>2</sup>) for 10 min without pressure followed by 3 min under 15 MPa of pressure. They were then removed from the mold and cooled at ambient temperature. The resulting films were about 0.5 mm thick.

#### Water Vapor Sorption Analysis

WG powder and square samples cut from the films (approximately 1 × 1 cm<sup>2</sup>) were first conditioned into a desiccator containing silica gel at room temperature until constant weight was reached (about 3 days). After the measurement of the initial dry weight ( $W_i$ ), three replicates per sample were stored at 20°C into desiccators containing saturated salt solutions of CaCl<sub>2</sub>, K<sub>2</sub>CO<sub>3</sub>, NaBr, NaCl, KCl and K<sub>2</sub>SO<sub>4</sub> producing relative humidity respectively of 35, 43, 58, 75, 88, and 98%.<sup>37</sup> When equilibrium was reached after two successive equal weighings (about 1 week), the equilibrium weight ( $W_{eq}$ ) was measured. After equilibrium, the samples were dried again over silica gel and the final weight ( $W_f$ ) was measured. The water content  $m_w$  was calculated as:

$$m_w (\text{wt } \%, \text{ wet basis}) = 100 \times \frac{W_{eq} - W_f}{W_{eq}} \quad (1)$$

At high relative humidity (88 and 98% RH), droplets resulting from water condensation or plasticizer exudation were found on the surface of the films. Therefore, the surfaces were carefully wiped with absorbing paper before measuring the film mass. In consequence,  $W_f$  was found lower than  $W_p$  as a result of a loss of glycerol, rising doubt on the accuracy of the material water determination above 88% RH.

#### Dynamic Mechanical Analysis (DMA)

Prior to the analysis, the samples were equilibrated at 0, 43 or 75% RH. DMA was performed on a RSA II Solids Analyzer (Rheometrics) testing machine in tensile mode at a frequency of 1 Hz with 0.01% strain amplitude. Analyses were performed on rectangular samples from -90 to 150°C at a heating rate of 3°C/min. The samples dimensions were measured each time with a caliper on five different points (approximately 20 × 10 × 0.5 mm<sup>3</sup>). Storage modulus ( $E'$ ), loss modulus ( $E''$ ) and  $\tan \delta$  ( $=E''/E'$ ) were continuously recorded during the experiment. Each sample was analyzed in triplicate.

## RESULTS AND DISCUSSION

#### Characterization of WG and Its Fractions

The protein content of the initial WG has been found to be 76.4 wt % on dry basis, a value in the range of other literature data.<sup>38,39</sup> Among those proteins, 56 wt % are gliadins and 44 wt % are glutenin (Table I). The residual starch content is quite high (19.4 wt %). The remaining material is most likely to be lipids, whose amount in WG is usually around a few percent.

The results of the fractionation of the initial WG into gliadin-rich and glutenin-rich fractions are reported in Table I. The total mass recovery after fractionation is only 80 wt %, because of losses of soluble material during the washing steps with water. The gliadin-rich fraction contains 85.2 wt % gliadins and negligible amount of starch, while the glutenin-rich fraction is composed of 63.1 wt % glutenins, and still contains 7.5 wt % starch. Most of the starch initially present in gluten has thus been lost during the washing steps of the protein fractions.

#### Influence of Glycerol on the Water Vapor Sorption of WG Materials

Water vapor sorption isotherms of the native gluten and WG materials including variable glycerol contents are presented in Figure 1. As glycerol is a very hydrophilic compound, its incorporation into the materials leads to an increase in the amount of absorbed water compared to the native gluten.<sup>19,20,40</sup> The addition of hydrophilic plasticizers to biopolymers has been

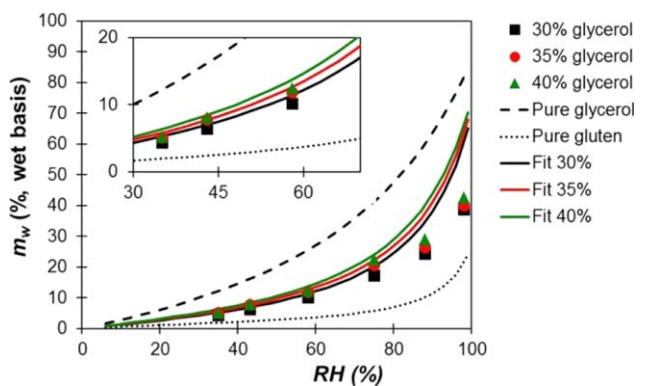


**Figure 1.** Water vapor sorption isotherms of gluten materials plasticized with 30, 35, or 40 wt % glycerol (symbols). Error bars are included in the symbols. Continuous lines present the fit of the experimental data according to a simple mixing law between native gluten (dotted line) and pure glycerol (dashed line, data from Marcolli & Peter<sup>42</sup>). [Color figure can be viewed in the online issue, which is available at [wileyonlinelibrary.com](http://wileyonlinelibrary.com).]

shown to influence the water vapor sorption in two stages.<sup>41,42</sup> Low amounts of plasticizers (< 10–20 wt %) occupy the first hydration shell of the biopolymer, thus competing for water sorption at low RH. This is typically the case for carbohydrate and protein-based biomaterials including less than 20 wt % glycerol which showed reduced water absorption.<sup>41,42</sup> For higher amounts of plasticizers, as it is the case in this study, the water vapor sorption increases with the plasticizer content, because the plasticizer itself can contribute to water absorption.<sup>42</sup>

Because the materials include more than 20 wt % glycerol, we hypothesized that gluten and glycerol contribute independently to the moisture sorption. Taking into account the moisture sorption behaviors of native gluten measured in this study and literature data for pure glycerol,<sup>43</sup> theoretical sorption values of the materials were calculated considering a simple additive mixing law:

$$m_{w, th} = x_{gly}m_{w, gly} + x_{glu}m_{w, glu} \quad (2)$$

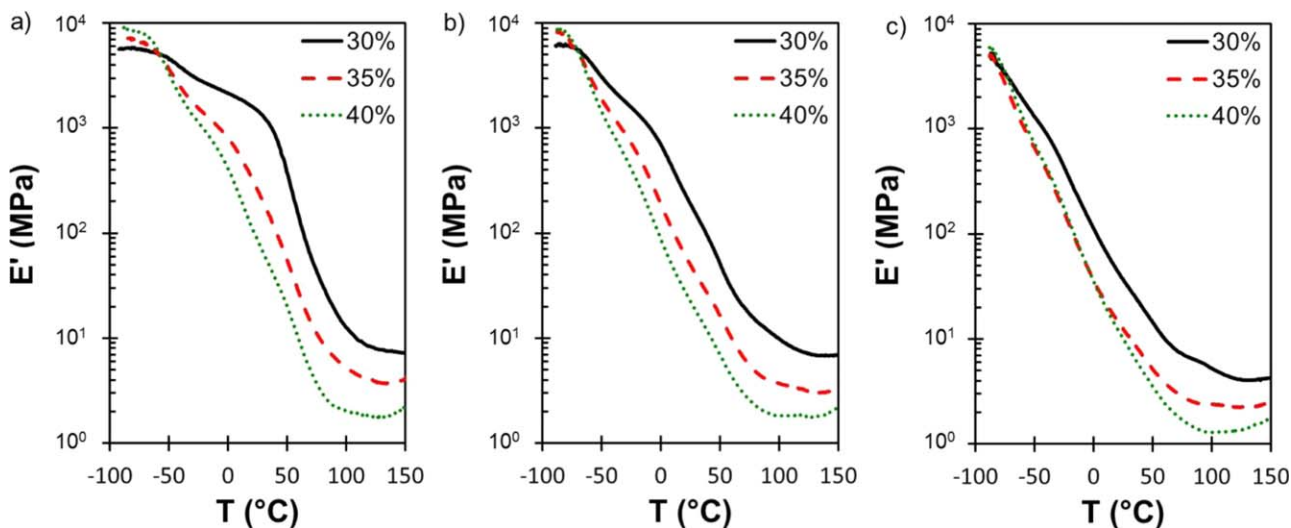


**Figure 2.** Storage modulus  $E'$  of wheat gluten materials plasticized by 30, 35, or 40 wt % glycerol, after storage at 0 (a), 43 (b), or 75% RH (c). [Color figure can be viewed in the online issue, which is available at [wileyonlinelibrary.com](http://wileyonlinelibrary.com).]

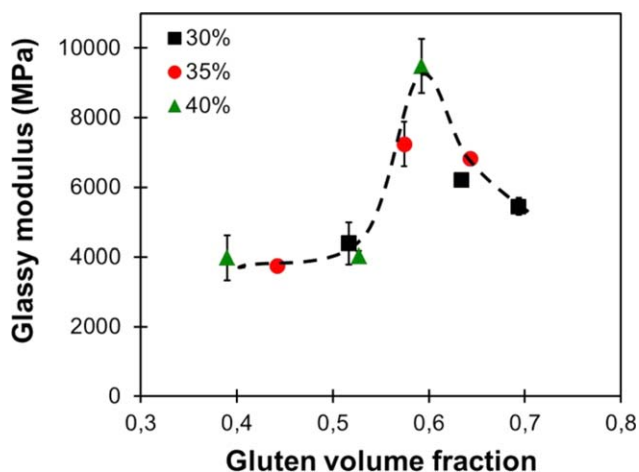


**Figure 3.** Materials glassy modulus depending on the gluten volume fraction. Glassy modulus was taken at  $-80^{\circ}\text{C}$ . [Color figure can be viewed in the online issue, which is available at [wileyonlinelibrary.com](http://wileyonlinelibrary.com).]

where  $x_{gly}$  and  $x_{glu}$  represent the mass fractions of glycerol and gluten in the materials, and  $m_{w, gly}$  and  $m_{w, glu}$  the absorbed water by each component at the corresponding RH.

The calculated values, presented as continuous lines in Figure 1, fit correctly the experimental data up to 75% RH. For  $\text{RH} \geq 88\%$ , plasticizer exudation impaired the exact determination of the equilibration moisture, causing the observed deviation from the simple mixing rule.

#### DMA of WG Materials: Influence of Glycerol and Water on the Glassy and Rubbery Moduli

DMA was performed on materials containing 30–40 wt % glycerol after storage at 0, 43, or 75% RH. Figure 2 represents the evolution of the storage modulus  $E'$  as a function of the temperature, depending on the glycerol content.

The values of  $E'$  on the glassy modulus were collected, and are plotted on Figure 3 against the gluten volume fraction of the

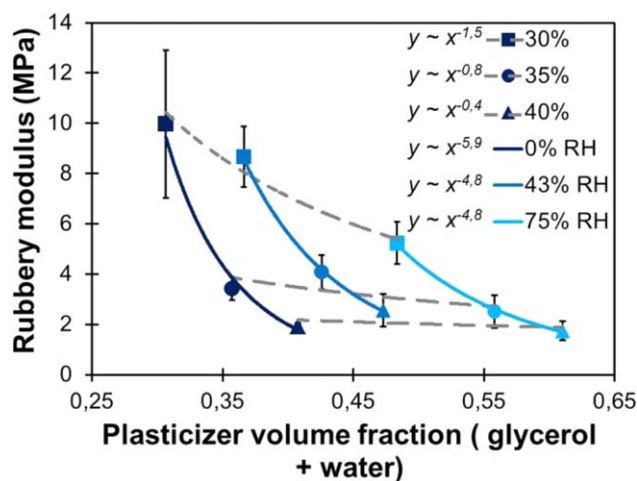


**Figure 4.** Materials rubbery modulus depending on the total volume fraction of plasticizer (glycerol + water). Data are gathered in series according to either their glycerol content (symbols shape) or equilibrium moisture (fillings series) and fitted to power laws. Rubbery modulus was taken at 120°C. [Color figure can be viewed in the online issue, which is available at [wileyonlinelibrary.com](http://wileyonlinelibrary.com).]

materials. Important variations are observed according to both glycerol and water content. It appears that an optimum seems to exist at about 60 vol % of gluten, where the glassy modulus culminates. Combination of greater closeness of interacting protein chains and minimization of void defects results in glassy modulus optimum. Full gluten plasticization during material processing is needed in order to obtain a well condensed material. In that respect glycerol plays a double role: it acts as a solvent phase allowing the saturation of the dry gluten particles, and at a molecular level it is going to plasticize proteins, allowing the formation of interactions favoring the material cohesiveness.

Similarly, the value of  $E'$  on the rubbery plateau was analyzed. It can clearly be seen from Figure 2 that an increase in the glycerol content lowers the rubbery modulus, as previously reported by Pommet *et al.*<sup>21</sup> This phenomenon could arise from a simple “dilution” effect, since the increase in plasticizer causes the volume fraction of polymer chains to decrease. But polymer concentration drop could also negatively impact gluten crosslinking during processing. Both features might contribute to the decrease of the gluten material rubbery modulus.<sup>31</sup>

To clarify this point the rubbery modulus of all materials were plotted against the total plasticizer (glycerol + water) volume fraction (Figure 4). The “dilution” effect of the plasticizer on  $E'$  modulus can be judged by following the impact of the water increase within each glycerol series (Figure 4, same symbols, dotted fitting line). For 35 and 40% glycerol, the rubbery modulus remains constant with the increase in water content, whereas it slightly decreases for 30% glycerol, following a power law with exponent  $-1.5$ . At a given RH, the effect of an increase in glycerol content led to much more pronounced decays, with power exponents ranging from  $-4.8$  to  $-5.9$  (Figure 4, continuous fitting line). The stronger influence of glycerol on the elastic modulus should then be related to a depressing

effect on the protein crosslinking during material thermoforming at 120°C.

#### DMA of WG Materials: Influence of Glycerol and Water on the Glass Transition

To evaluate the glass transition of the materials at different glycerol and water content, the evolution of the loss factor  $\tan \delta$  with the temperature was considered. Figure 5 shows the  $\tan \delta$  curves measured on the WG materials containing 30–40 wt % glycerol, after storage at 0, 45 or 75% RH. A global shift of the curves toward lower temperature is observed when the relative humidity increases, i.e., when the water content of the materials is higher, confirming the ability of water to participate in WG plasticization.<sup>22,44,45</sup>

The curves of the loss factor  $\tan \delta$  present a particular shape, with two distinct peaks: one around  $-60^\circ\text{C}$ , the other one at about  $70^\circ\text{C}$ . This is characteristic of the coexistence of two phases inside the materials, each one relaxing at different temperatures,<sup>26</sup> a phenomenon already well described in glycerol-plasticized biopolymers. A transition at low temperature has already been described with e.g., gluten<sup>46,47</sup>, soy protein isolate,<sup>48–51</sup> starch,<sup>41,52,53</sup> amylose<sup>54,55</sup> and amylopectin,<sup>56</sup> or chitosan,<sup>57</sup> using either DMA or DSC. Its appearance was found to be related to critical glycerol content, e.g. 15 wt % or 25 wt % glycerol for gliadin<sup>58</sup> and soy-based materials,<sup>50</sup> respectively. In consequence this low- $T$  glass transition is assigned to the formation of glycerol-rich domains and interpreted as the evidence of a low compatibility between glycerol and the biopolymer.<sup>46,47</sup> This phase always coexists with another one that relaxes at higher temperature, and is thought to be composed mainly of the biopolymer.

On the main peak, a shoulder is visible for all materials except the dry material containing only 30 wt % glycerol. This kind of  $\tan \delta$  curve shape has been reported several times in the literature for WG-based materials,<sup>46,47,59,60</sup> though without being clearly discussed. The existence of an intermediate third phase has been postulated for soy protein and gluten-based materials, based on the observation of an additional transition close to  $0^\circ\text{C}$  either by DSC<sup>51</sup> or DMA.<sup>47</sup> In both cases it was observed only for hydrated samples, which led the authors to postulate the occurrence of protein domains that can only be plasticized by water. Our results are in striking contrast, since this transition is also observed on anhydrous samples, as long as the glycerol content exceeds 30 wt %.

The positions and heights of the low- and high- $T$  peaks and the shoulder on the  $\tan \delta$  curves are reported as a function of the water content on Figure 6. Both the low- and high- $T_g$  decrease when the water content increases. Interestingly, the  $T_g$  of the glycerol-rich phase is independent on the material glycerol content. Similar observation has been done on glycerol-plasticized starch, amylose or amylopectine.<sup>52,56</sup> This implies that the glycerol-rich phase has a constant composition, whatever the total glycerol content. The net increase of the peak area involves that its volume fraction increases with the bulk water content [Figure 6(b)].

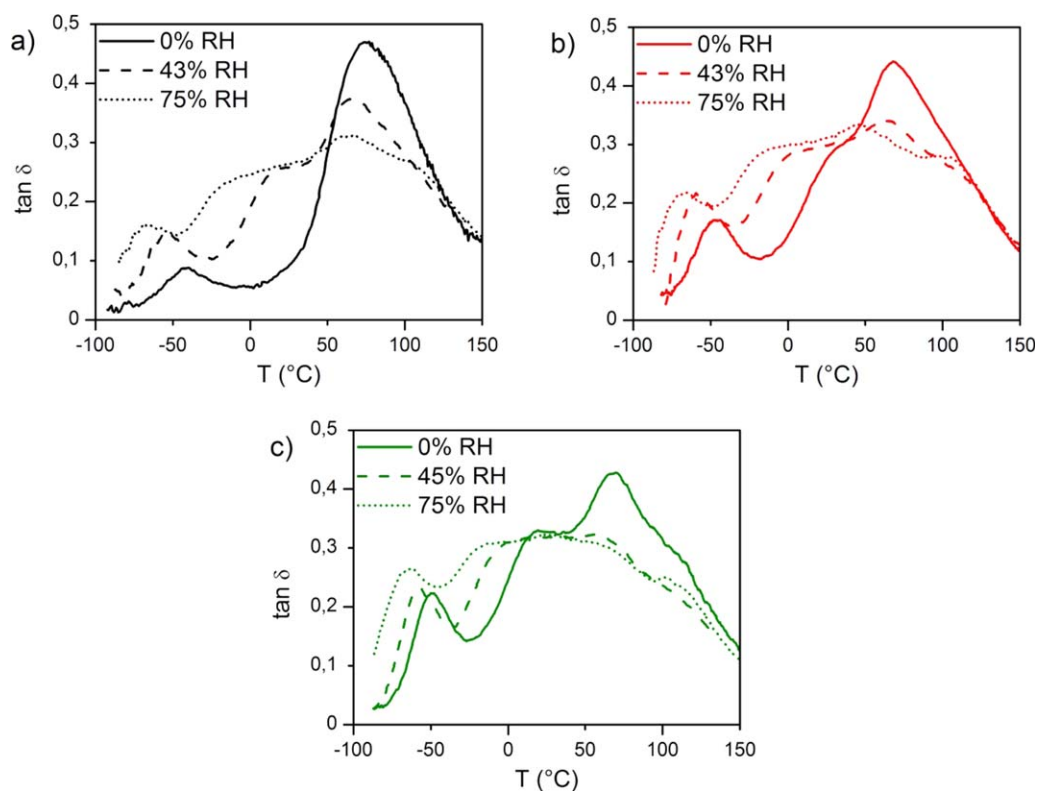


**Figure 5.** Loss factor  $\tan \delta$  depending on the relative humidity of storage of gluten materials plasticized by 30 (a), 35 (b), and 40 wt % glycerol (c). [Color figure can be viewed in the online issue, which is available at [wileyonlinelibrary.com](http://wileyonlinelibrary.com).]

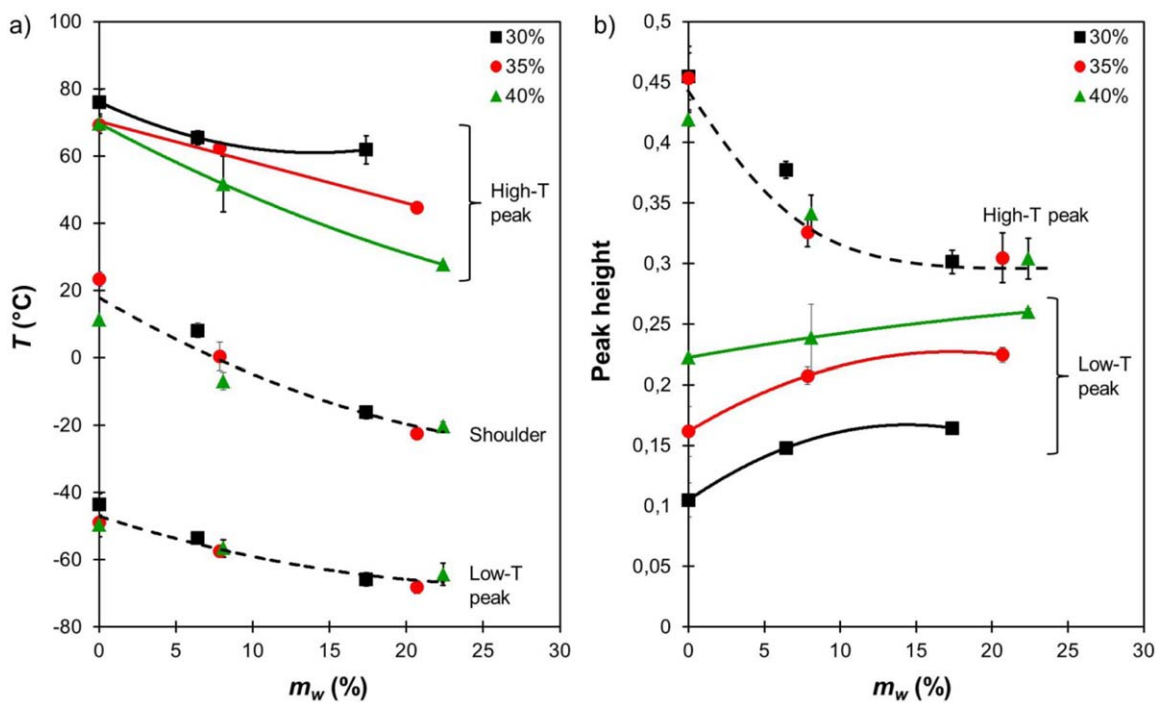


**Figure 6.** Temperatures of the high- and low-T peaks and the shoulder on the  $\tan \delta$  curves (a) and height of the  $\tan \delta$  peaks (b) as measured by DMA, depending on the glycerol (30, 35, or 40 wt %) and water content of the materials. [Color figure can be viewed in the online issue, which is available at [wileyonlinelibrary.com](http://wileyonlinelibrary.com).]

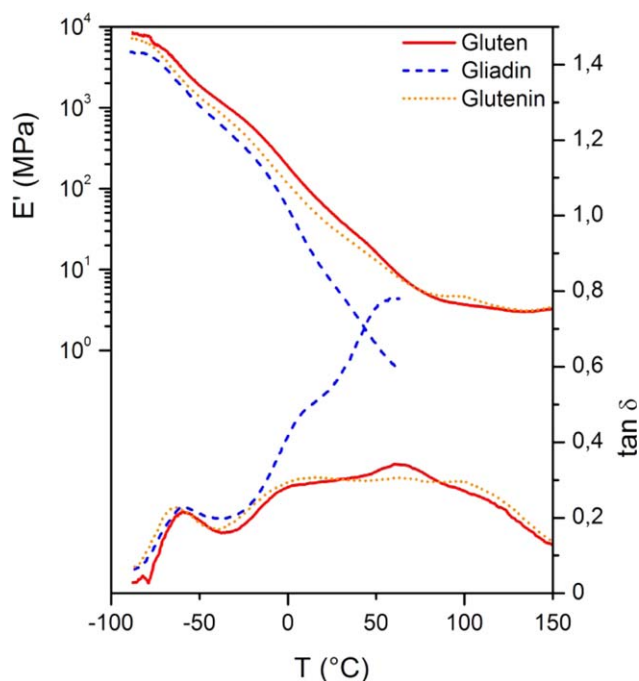


**Figure 7.** Storage modulus  $E'$  and loss factor  $\tan \delta$  of protein materials plasticized by 35 wt % glycerol after storage at 43% RH. [Color figure can be viewed in the online issue, which is available at [wileyonlinelibrary.com](http://wileyonlinelibrary.com).]

On the other hand, the  $T_g$  of the gluten-rich phase depends on both water and glycerol contents, an augmentation of any of these inducing a decrease in  $T_g$ . Its peak height appears to be independent on the total glycerol content. When the water content increases, this peak broadens, causing the peak height to decrease and reach a plateau value of approximately 0.3.

#### DMA of WG Materials: Influence of the Type of Protein

Gluten is composed of a complex mixture of two types of protein, gliadins and glutenins. Confocal microscopy observations suggested a possible phase separation between them in WG-based materials.<sup>61</sup> Such phase separation could also be responsible for the complex shape of the  $\tan \delta$  curves of the materials, if both proteins relax at different temperatures.

To question this hypothesis, materials have been prepared using the gliadin- and glutenin-rich fractions. The DMA curves of those materials containing 35 wt % glycerol are shown in Figure 7. The behaviors of gluten and glutenin materials are very similar. Indeed, their compositions are not so different (Table I). The behavior of the gliadin-rich fraction is on the other hand very different. The drop in modulus is much more pronounced, to the extent that the measurement cannot be conducted at temperatures above  $T_g$ . Gliadins are not crosslinked in the native state, and even though some temperature-induced crosslinking can take place, materials prepared with gliadins always have a lower crosslinking density than those prepared with gluten or glutenins.<sup>31</sup> It seems here that the materials prepared with the gliadin-rich fraction are not crosslinked enough to provide enough mechanical strength above  $T_g$ , which explains that the rubbery plateau cannot be observed.

The low-T peak on the  $\tan \delta$  curves is almost unchanged, because all the materials have the same glycerol content. The temperature of the main peak is in the same range for all materials, and the shoulder on the main peak exists for both the gliadin-rich and the glutenin-rich fraction. The height of the main peak is much greater for gliadins than for glutenins, but it only results from the violent drop in  $E'$  modulus caused by the low crosslinking density of the gliadins. Thus, it doesn't seem that the complex shape of the  $\tan \delta$  curves can be attributed to a distinct behavior of the two main gluten protein classes, gliadin and glutenin. It is more likely to result from a complex distribution of the plasticizer inside the materials, as will be discussed below.

#### Phase Separation and Multiple Relaxations in Glycerol-Plasticized WG

If the existence of several phases in plasticized WG is well established, their composition has never been discussed in details. Here, we estimated the composition of both glycerol- and gluten-rich phases, using Couchman-Karas (C – K) equation.<sup>25</sup> We first limited to the case where the system is only bi-component, i.e., to dry samples only containing glycerol and gluten. C–K equation is widely used to evaluate the glass transition temperature of a mixture of polymers, or polymer and plasticizer. It relates the observed  $T_g$  of the blend to the glass transition and heat capacity increment of the individual components,  $T_{gi}$  and  $\Delta c_{pi}$ :

$$T_g = \frac{x_1 T_{g1} \Delta c_{p1} + x_2 T_{g2} \Delta c_{p2}}{x_1 \Delta c_{p1} + x_2 \Delta c_{p2}} \quad (3)$$

with subscript 1 and 2 referring respectively to gluten and glycerol.

The individual glass transition temperatures can be measured or taken from the literature. The measurement of the  $T_g$  of the blend over a wide range of composition allow to determine the  $\Delta c_{pi}$  by fitting the data. This approach allowed Pouplin *et al.*<sup>22</sup> and Kalichevsky *et al.*<sup>62</sup> to obtain a value of  $\Delta c_p$  equal to 0.40 for WG. The same value was later obtained by van der Sman on numerous biopolymers.<sup>63</sup>

Accounting that both  $T_{gi}$  and  $\Delta c_{pi}$  are known, and that  $x_2 = 1 - x_1$ , the measurement of the  $T_g$  of a phase can then allow to calculate its composition, by a rearrangement of C – K equation:

$$x_1 = \frac{\Delta c_{p2} (T_{g2} - T_g)}{\Delta c_{p2} (T_{g2} - T_g) - \Delta c_{p1} (T_{g1} - T_g)} \quad (4)$$

This calculation has been used to evaluate the composition of the glycerol-rich and gluten-rich phases of the dried materials. In the presence of water, the extended C–K equation can be used, to take into account the three components of the system<sup>26,27</sup>:

$$T_g = \frac{x_1 \Delta c_{p1} T_{g1} + x_2 \Delta c_{p2} T_{g2} + x_3 \Delta c_{p3} T_{g3}}{x_1 \Delta c_{p1} + x_2 \Delta c_{p2} + x_3 \Delta c_{p3}} \quad (5)$$

with the additional subscript 3 referring to water.

Considering that the simple additive mixing law applies within the RH range studied, the water content  $x_3$  can be written as:

**Table II.** Volume Fraction of Gluten, Glycerol and Water in the Three Different Phases

Total glycerol (%)	RH (%)	Glycerol-rich phase				Intermediate phase				Gluten-rich phase			
		$T_g$ (°C)	$v_{gluten}$	$v_{glycerol}$	$v_{water}$	$T_g$ (°C)	$v_{gluten}$	$v_{glycerol}$	$v_{water}$	$T_g$ (°C)	$v_{gluten}$	$v_{glycerol}$	$v_{water}$
30	0	-43.6	0.32 ± 0.02	0.68 ± 0.05	-	-	-	-	-	76.1	0.78 ± 0.04	0.22 ± 0.01	-
	43	-53.5	0.33 ± 0.01	0.55 ± 0.02	0.12 ± 0.00	8.1	0.63 ± 0.03	0.28 ± 0.01	0.09 ± 0.00	65.4	0.80 ± 0.03	0.13 ± 0.00	0.06 ± 0.00
	75	-65.9	0.36 ± 0.02	0.41 ± 0.02	0.24 ± 0.01	-16.2	0.59 ± 0.02	0.23 ± 0.01	0.17 ± 0.01	61.8	0.83 ± 0.05	0.07 ± 0.00	0.10 ± 0.00
35	0	-48.9	0.29 ± 0.03	0.71 ± 0.07	-	23.3	0.61 ± 0.02	0.39 ± 0.01	-	69.3	0.76 ± 0.02	0.24 ± 0.01	-
	43	-57.5	0.34 ± 0.01	0.52 ± 0.02	0.14 ± 0.00	0.4	0.61 ± 0.05	0.30 ± 0.02	0.09 ± 0.00	62.5	0.79 ± 0.01	0.14 ± 0.00	0.06 ± 0.00
	75	-68.3	0.34 ± 0.02	0.41 ± 0.02	0.24 ± 0.01	-22.5	0.57 ± 0.02	0.26 ± 0.01	0.17 ± 0.01	44.5	0.80 ± 0.02	0.10 ± 0.00	0.10 ± 0.00
40	0	-49.6	0.29 ± 0.01	0.71 ± 0.01	-	11.3	0.57 ± 0.00	0.43 ± 0.00	-	69.7	0.76 ± 0.00	0.24 ± 0.00	-
	43	-56.7	0.35 ± 0.02	0.51 ± 0.03	0.14 ± 0.01	-6.9	0.58 ± 0.03	0.32 ± 0.02	0.10 ± 0.00	51.6	0.77 ± 0.10	0.16 ± 0.02	0.06 ± 0.01
	75	-64.4	0.37 ± 0.03	0.40 ± 0.03	0.23 ± 0.02	-20.3	0.58 ± 0.02	0.25 ± 0.01	0.17 ± 0.00	27.7	0.74 ± 0.01	0.13 ± 0.00	0.13 ± 0.00

Calculation based on eq. (7).

$$x_3 = \alpha x_1 + \beta x_2 \quad (6)$$

where  $\alpha$  and  $\beta$  respectively represent the water absorption of native gluten and pure glycerol at the corresponding RH.

Equation (5) can then be rewritten to calculate the phase composition in presence of water:

$$x_1 = \frac{A [\Delta c_{p2}(T_g - T_{g2}) + B\Delta c_{p3}(T_g - T_{g3})]}{\Delta c_{p1}(T_{g1} - T_g) - B\Delta c_{p2}(T_{g2} - T_g) + (B - 1)\Delta c_{p3}(T_{g3} - T_g)} \quad (7)$$

with  $A = 1/(1 + \beta)$  and  $B = (1 + \alpha)/(1 + \beta)$ . In the absence of water,  $\alpha = \beta = 0$ , hence  $A = B = 1$ , and eq. (6) reduces to eq. (3). For glycerol and water,  $\Delta c_p$  and  $T_g$  were respectively taken as 0.88 and 1.94 J g<sup>-1</sup> K<sup>-1</sup>, and 180 and 134 K.<sup>22,64</sup>

The mass fractions  $x_i$  calculated with eqs. (5) or (7) was subsequently converted into volume fractions  $v_i$  using densities of 1.31, 1.26 and 1 for gluten, glycerol and water respectively, and compiled in Table II.

The glycerol-rich phase presents a very low protein volume fraction (30–35 vol %), which as showed by the linear regression in Figure 8 significantly tends to increase with the bulk water content of the materials (Pearson p-value 0.009).

Relationship in Figure 8 demonstrates that the glycerol-rich phase significantly grew denser while the bulk water content of

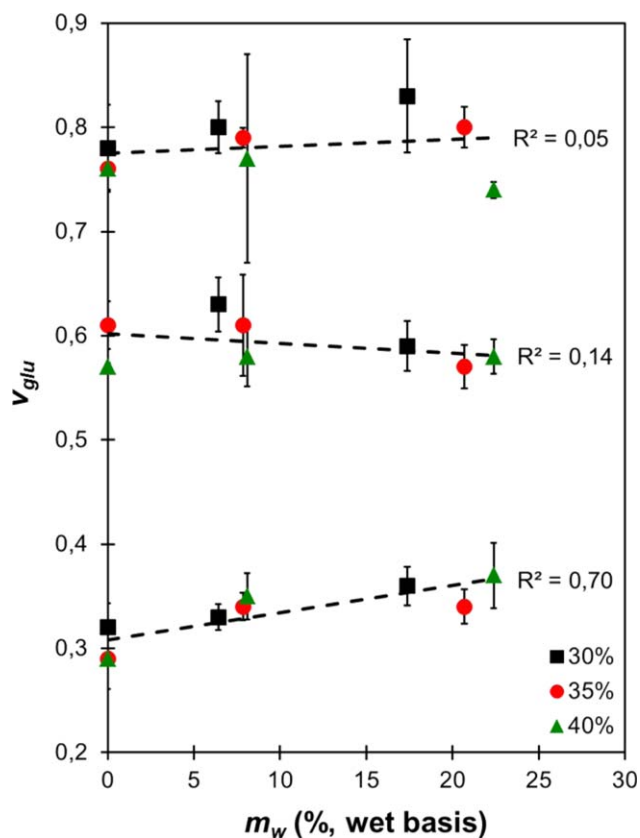


**Figure 8.** Evolution of the volume fraction of gluten ( $v_{glu}$ ) in the different phases with the material water content, as a function of the glycerol content. [Color figure can be viewed in the online issue, which is available at wileyonlinelibrary.com.]



the materials increases. Indeed, the replacement of glycerol by smaller water molecules (about  $30 \text{ \AA}^3$  against  $121 \text{ \AA}^3$ ) in the vicinity of the protein causes the protein chains to become more densely packed.

The low protein volume fraction suggests that the first thermal relaxation could correspond to the vibrational and rotational motions of the side groups of the amino-acids located at the vicinity of the protein surface. Most of the side groups protruding from the protein surface strongly interact through H-bonds with plasticizer molecules. In the context of water vapor sorption, the first hydration layer composed of water molecules directly H-bonded to the surface polar groups of proteins commonly accounts for 0.3–0.35 g water/g protein.<sup>65</sup> For protein in water solution, the hydration shell extends to several molecular layers of water, so that 1 g of protein is being more or less slaved to 1–1.2 g of water.<sup>66</sup> Long-range interactions between proteins and their collective behavior derived from the presence of the hydration shells. As the material temperature raises, density fluctuation of plasticizer molecules increase and cooperatively trigger that of the polar groups they are connected to.

The intermediate  $\tan \delta$  peak corresponds to a phase packed at  $59 \pm 2 \text{ vol } \%$ . This value is close to the bulk gluten volume fraction leading to the highest vitreous elastic modulus (Figure 3). On a macroscopic scale, the relaxation of the intermediate phase coincided with an  $E'$  modulus drop by 10 decades, attesting for its strong implication in the glass to rubbery transition of the bulk materials. In addition, the prevalence of the intermediate phase was relatively more important for glutenin-based materials than for gliadins (Figure 7). It is well established that glutenin polymers are the most reactive during thermal treatment: they aggregate through disulfide inter-chains cross-links before gliadins, which, in turn, became linked to the latter.<sup>35</sup> It thus seems that the intermediate relaxation arises from the cooperative and collective motions of proteins optimally packed at 60 vol %, and permanently connected by disulfide cross-linking. More than 30 vol % of plasticizer was compulsory for observing the relaxation of this protein phase at intermediate-temperature.

The third transition corresponds to a highly packed protein fraction, from 74 to 83 vol % (Table II). At the highest RH studied and on a mass basis, this phase includes more water than glycerol. Following the argument developed by Copolla *et al.*<sup>67</sup> and more recently by Van der Sman,<sup>63</sup> we hypothesized that 0.66 mol glycerol will be as effective as 1 mol water to plasticize protein, since glycerol possesses three OH groups while water can be viewed as bearing two equivalent OH groups, considering the ubiquitous H-bonding capability of its two hydrogen atoms. In terms of mass, this corresponds to consider 3.4 g glycerol to be as effective as 1 g water. Assuming this equivalence between both plasticizers, we calculated the equivalent weight of water that would account for the plasticizers effect of both glycerol and water. On average, it leads to a water-to-protein ratio of 0.117 g/g. This amount is larger than the first monomolecular water layer interacting with the protein backbone (0.045 g/g), and could coincide to the 2D percolation transition of the water molecules involved in the first layer of

the protein hydration shell. Such percolation threshold was detected for several globular proteins within the range of 0.13–0.18 g of water per g dry protein.<sup>68,69</sup> Local percolation of the water molecules interacting with the polar groups of the protein surface would trigger protein segmental movements and would allow for protein conformational mobility.

We can resume our findings considering the exemplary behavior of the dry material including only 30 wt % glycerol. At this gluten - glycerol mass ratio, the protein volume fraction is high, a situation which favors the formation of permanent disulfide cross-links during material processing. On the other hand, the plasticizer content would be too low to insure the saturation of all the WG proteins at the previously discussed optimal packing volume fraction of 60 vol %. The material would present internal defects in the form of nanoscopic to microscopic voids that are going to weaken the glassy modulus. Nevertheless, at 30 wt % glycerol, there would be enough plasticizer to insure the 2D percolation of most of the protein solvation shells and to allow the filling of some of the nanoscale voids. Material mechanical relaxation will thus involve only two processes. At the low-temperature side the glycerol molecules gathered within the voids will be the first to experience collective dynamic motion. Through long-range interactions they will trigger vibration and bending motion of the amino-acid side-groups located at their vicinity. Because of the limited amount of glycerol, the saturation of the protein aggregates packed at 60% will not be possible. In the absence of the liquid diluent phase, compulsory for the onset of the collective diffusional motion of gluten aggregates, no distinct intermediate relaxation process will be recorded. Instead, and at the upper-temperature side, a mechanical relaxation peak driven by a 2D network of plasticizer molecules H-bonded to the protein surface and related to the conformational mobility of the protein is recorded.

## CONCLUSIONS

The multiple relaxation peaks observed in  $\tan \delta$  curves point to a hierarchical organization of plasticizer molecules. Plasticizers play a crucial role for triggering the dynamic relaxation of protein at different scales. The low-temperature side transition would correspond to a transition mainly involving plasticizer molecules H-bonded to the protein surface and gathered into nanoscale voids. The higher temperature relaxation process would reflect the conformational mobility of the protein triggered by a 2D network of interacting plasticizer molecules located at the surface of the protein. The intermediate relaxation process would emerge above critical plasticizer content, higher enough to saturate clusters of strongly interacting proteins. In that case it relies on their collective diffusional motion.

## ACKNOWLEDGMENTS

This project was conducted thanks to a grant from la Région Rhône-Alpes. Tereos Syral is gratefully acknowledged for graciously providing the wheat gluten used in this study. The authors would also like to thank Joëlle Bonicel (IATE) for her help while performing the SE-HPLC analysis of proteins.

## REFERENCES

1. Belgacem, M. N.; Gandini, A. *Monomers, Polymers and Composites From Renewable Resources*; Elsevier: Amsterdam, **2008**.
2. Gandini, A. *Green Chem.* **2011**, *13*, 1061.
3. Reddy, N.; Yang, Y. *J. Appl. Polym. Sci.* **2013**, *130130*, 729.
4. Hernandez-Izquierdo, V. M.; Krochta, J. M. *J. Food Sci.* **2008**, *73*, R30.
5. Zhang, H.; Mittal, G. *Environ. Prog. Sustain. Energy* **2010**, *29*, 203.
6. Feillet, P. *Le grain de blé, composition et utilisation*; INRA Editions, **2000**.
7. Müller, S.; Wieser, H. *J. Cereal. Sci.* **1995**, *22*, 21.
8. Wieser, H. *Food Microbiol.* **2007**, *24*, 115.
9. Shewry, P. R.; Tatham, A. S.; Forde, J.; Kreis, M.; Mifflin, B. *J. J. Cereal Sci.* **1986**, *44*, 97.
10. Shewry, P. R.; Halford, N. G.; Belton, P. S.; Tatham, A. S. *Philos. Trans. R. Soc. B Biol. Sci.* **2002**, *357*, 133.
11. Noel, T. R.; Parker, R.; Ring, S. G.; Tatham, A. S. *Int. J. Biol. Macromol.* **1995**, *17*, 81.
12. Abdellatif, A. M.; Alruqaie, I. M.; Alamri, M. S.; Shahzad, H. *J. Food Agric. Environ.* **2013**, *11*, 477.
13. Micard, V.; Belamri, R.; Morel, M. H.; Guilbert, S. *J. Agric. Food Chem.* **2000**, *48*, 2948.
14. Immergut, E. H.; Mark, H. F. In *Plasticization and Plasticizer Processes*; *Advances in Chemistry*; American Chemical Society: Washington D.C., **1965**; Vol. 48, pp 1–26.
15. Vieira, M. G. A.; da Silva, M. A.; Santos, L. O.; dos, Beppu, M. M. *Eur. Polym. J.* **2011**, *47*, 254.
16. Mangavel, C.; Rossignol, N.; Perronnet, A.; Barbot, J.; Popineau, Y.; Guéguen, J. *Biomacromolecules* **2004**, *55*, 1596.
17. Pan, Y.; Wang, X.; Yuan, Q. *J. Appl. Polym. Sci.* **2011**, *121*, 797.
18. Gällstedt, M.; Mattozzi, A.; Johansson, E.; Hedenqvist, M. S. *Biomacromolecules* **2004**, *55*, 2020.
19. Gontard, N.; Guilbert, S.; Cuq, J. L. *J. Food Sci.* **1993**, *58*, 206.
20. Angellier-Coussy, H.; Torres-Giner, S.; Morel, M. H.; Gontard, N.; Gastaldi, E. *J. Appl. Polym. Sci.* **2008**, *107*, 487.
21. Pommet, M.; Redl, A.; Guilbert, S.; Morel, M. H. *J. Cereal Sci.* **2005**, *42*, 81.
22. Pouplin, M.; Redl, A.; Gontard, N. *J. Agric. Food Chem.* **1999**, *47*, 538.
23. Irissin-Mangata, J.; Bauduin, G.; Boutevin, B.; Gontard, N. *Eur. Polym. J.* **2001**, *37*, 1533.
24. Pommet, M.; Redl, A.; Morel, M. H.; Guilbert, S. *Polymer* **2003**, *44*, 115.
25. Couchman, P. R.; Karasz, F. E. *Macromolecules* **1978**, *11*, 117.
26. Belfiore, L. A. In *Physical Properties of Macromolecules*; John Wiley & Sons, Inc., Hoboken (NJ) **2010**; pp 1–47.
27. Bhandari, B.; Adhikari, B. In *Advances in Food Dehydration*; Ratti, C., Ed.; CRC Press: Boca Raton, FL, **2009**.
28. Schofield, J. D.; Bottomley, R. C.; Timms, M. F.; Booth, M. R. *J. Cereal Sci.* **1983**, *11*, 241.
29. Morel, M. H.; Redl, A.; Guilbert, S. *Biomacromolecules* **2002**, *33*, 488.
30. Auvergne, R.; Morel, M. H.; Menut, P.; Giani, O.; Guilbert, S.; Robin, J. J. *Biomacromolecules* **2008**, *99*, 664.
31. Redl, A.; Guilbert, S.; Morel, M. H. *J. Cereal Sci.* **2003**, *38*, 105.
32. Lagrain, B.; Thewissen, B. G.; Brijs, K.; Delcour, J. A. *Food Chem.* **2008**, *107*, 753.
33. Chen, L.; Reddy, N.; Wu, X.; Yang, Y. *Ind. Crops Prod.* **2012**, *35*, 70.
34. Jarvis, C. E.; Walker, J. R. L. *J. Sci. Food Agric.* **1993**, *63*, 53.
35. Domenek, S.; Morel, M. H.; Bonicel, J.; Guilbert, S. *J. Agric. Food Chem.* **2002**, *50*, 5947.
36. Ferreira, S. P.; Ruiz, W. A.; Gaspar-Cunha, A. *Química Nova* **2012**, *35*, 719.
37. Nyqvist, H. *Int. J. Pharm. Technol. Prod. Manuf.* **1983**, *44*, 47.
38. Kunanopparat, T.; Menut, P.; Morel, M. H.; Guilbert, S. *Compos. Part A: Appl. Sci. Manuf.* **2008**, *39*, 777.
39. Jansens, K. J. A.; Lagrain, B.; Rombouts, I.; Brijs, K.; Smet, M.; Delcour, J. A. *J. Cereal Sci.* **2011**, *54*, 434.
40. Kayserilioğlu, B.; Bakir, U.; Yilmaz, L.; Akkaş, N. *J. Agric. Food Chem.* **2003**, *51*, 964.
41. Lourdin, D.; Coignard, L.; Bizot, H.; Colonna, P. *Polymer* **1997**, *38*, 5401.
42. Godbillot, L.; Dole, P.; Joly, C.; Rogé, B.; Mathlouthi, M. *Food Chem.* **2006**, *96*, 380.
43. Marcolli, C.; Peter, T. *Atmospheric Chem. Phys.* **2005**, *55*, 1545.
44. Gontard, N.; Ring, S. G. *J. Agric. Food Chem.* **1996**, *44*, 3474.
45. Zhang, X.; Do, M. D.; Hoobin, P.; Burgar, I. *Polymer* **2006**, *47*, 5888.
46. Zhang, X.; Burgar, I.; Do, M. D.; Loubakos, E. *Biomacromolecules* **2005**, *66*, 1661.
47. Sun, S.; Song, Y.; Zheng, Q. *Food Hydrocoll.* **2007**, *21*, 1005.
48. Huang, J.; Zhang, L.; Chen, F. *J. Appl. Polym. Sci.* **2003**, *88*, 3284.
49. Huang, J.; Zhang, L.; Chen, P. *J. Appl. Polym. Sci.* **2003**, *88*, 3291.
50. Chen, P.; Zhang, L. *Macromol. Biosci.* **2005**, *55*, 237.
51. Chen, P.; Zhang, L.; Cao, F. F. *Macromol. Biosci.* **2005**, *55*, 872.
52. Forssell, P. M.; Mikkilä, J. M.; Moates, G. K.; Parker, R. *Carbohydr. Polym.* **1997**, *34*, 275.
53. Teixeira, E. M.; Da Róz, A. L.; Carvalho, A. J. F.; Curvelo, A. A. S. *Carbohydr. Polym.* **2007**, *69*, 619.
54. Lourdin, D.; Bizot, H.; Colonna, P. *Macromol. Symp.* **1997**, *114*, 179.
55. Lourdin, D.; Ring, S. G.; Colonna, P. *Carbohydr. Res.* **1998**, *306*, 551.
56. Myllärinen, P.; Partanen, R.; Seppälä, J.; Forssell, P. *Carbohydr. Polym.* **2002**, *50*, 355.

57. Quijada-Garrido, I.; Iglesias-Gonzalez, V.; Mazon-Arechederra, J. M.; Barrales-Rienda, J. M. *Carbohydr. Polym.* **2007**, *68*, 173.
58. Sun, S.; Song, Y.; Zheng, Q. *J. Cereal Sci.* **2008**, *48*, 613.
59. Sun, S.; Song, Y.; Zheng, Q. *Food Hydrocoll.* **2008**, *22*, 1006.
60. Zárate-Ramírez, L. S.; Martínez, I.; Romero, A.; Partal, P.; Guerrero, A. *J. Sci. Food Agric.* **2011**, *91*, 625.
61. Kuktaite, R.; Plivelic, T. S.; Cerenius, Y.; Hedenqvist, M. S.; Gällstedt, M.; Marttila, S.; Ignell, R.; Popineau, Y.; Tranquet, O.; Shewry, P. R.; Johansson, E. *Biomacromolecules* **2011**, *12*, 1438.
62. Kalichevsky, M. T.; Jaroszkiewicz, E. M.; Blanshard, J. M. V. *Int. J. Biol. Macromol.* **1992**, *14*, 257.
63. van der Sman, R. G. M. *J. Phys. Chem. B* **2013**, *117*, 16303.
64. Orford, P. D.; Parker, R.; Ring, S. G.; Smith, A. C. *Int. J. Biol. Macromol.* **1989**, *11*, 91.
65. Kuntz, I. D. J.; Kauzmann, W. *Adv. Protein Chem.* **1974**, *28*, 239.
66. Sartor, G.; Hallbrucker, A.; Mayer, E. *Biophys. J.* **1995**, *69*, 2679.
67. Coppola, M.; Djabourov, M.; Ferrand, M. *Polymer* **2012**, *53*, 1483.
68. Careri, G.; Giansanti, A.; Rupley, J. A. *Proc. Natl. Acad. Sci.* **1986**, *83*, 6810.
69. Panagopoulou, A.; Kyritsis, A.; Sabater i Serra, R.; Gómez Ribelles, J. L.; Shinyashiki, N.; Pissis, P. *Biochim. Biophys. Acta* **2011**, *1814*, 1984.